



Enhanced DI Correlation Using WHWC Model Spanning the Visible and Near-Infrared Spectrum

Ratko Ivkovic^{1,2*}, Slobodan Bojanic Antonijevic³, Milos Stankovic¹, Aleksandar Markovic⁴, Zoran Milivojevic⁵ and Petar Spalevic⁶

¹Information Technology Department, MB University, Teodora Dražera 27, 11000, Belgrade, Serbia. ²Department of Software Engineering, Faculty of Economics and Engineering Management, University Business Academy in Novi Sad, Novi Sad, Serbia. ³Universidad Politécnica de Madrid, Madrid, Spain.

⁴Faculty of Sciences and Mathematics, University of Pristina in Kosovska Mitrovica, Kosovska Mitrovica, Serbia. ⁵Department for Information Technology, The Academy of Applied Technical and Preschool Studies, Nis, Serbia. ⁶Department of Electronic and Computer Engineering, Faculty of Technical Sciences, University of Pristina in Kosovska Mitrovica, Kosovska Mitrovica, Serbia. *Author for correspondence. E-mail: ratko.ivkovic@pr.ac.rs

ABSTRACT. Digital Image Correlation (DIC) is an advanced technique used for precise measurement of deformations, displacements, and strains on material surfaces through the analysis of digital images taken before and after loading. This paper introduces an alternative approach to DIC that integrates the Windowed Harmonic Weighted Correlation (WHWC) model, designed to improve accuracy and stability in the analysis of spectral images within the visible and near-infrared (NIR) spectrum. The WHWC model incorporates harmonic weighting and sinusoidal factors to enhance sensitivity to local changes, reduce the influence of noise, and maintain robustness across wavelengths ranging from 446 nm to 765 nm, covering both visible and NIR regions. Through experimental comparison with the Normalized Cross-Correlation (NCC) method, the WHWC model demonstrates significant improvements in stability and precision, achieving a correlation accuracy increase of 23% to 31%. The model was rigorously tested on a dataset of 600 spectral images, with results presented mathematically, visually, and descriptively, underscoring WHWC's capability for precise material analysis and reliable detection of subtle variations. These qualities position WHWC as a valuable tool in fields such as material science and biomedical imaging, where consistent, high-accuracy measurements are critical for structural analysis, environmental monitoring, and diagnostic imaging.

Keywords: Digital image processing; digital image correlation; visible spectrum; image quality evaluation.

Received on September 04, 2024.

Accepted on November 27, 2024.

Introduction

Digital Image Correlation (DIC) is a technique used to measure deformations, displacements, and strains on material surfaces through the analysis of digital images taken before and after loading. In the past three years, DIC technology has undergone significant advancements, both in theoretical and practical applications. The development of super-resolution digital image correlation (SR-DIC) has enabled the use of multiple low-resolution images to generate high-resolution images, allowing for more precise analysis of micro-level deformations. This technique has proven particularly useful in situations where traditional image stitching does not provide sufficient accuracy due to deformations or distortions (Hansen et al., 2021). Concurrently, the application of deep learning, especially convolutional neural networks (CNN), has significantly improved the accuracy and speed of DIC analyses, enabling faster and more robust predictions of displacement fields compared to traditional methods (Duan et al., 2023). The development of speckle patterns for DIC via 3D printing marked a significant step forward, as these optimized patterns enhanced the accuracy and repeatability of measurements, particularly in biomechanics and engineering applications (Yang et al., 2021). Additionally, the use of generative adversarial networks (GAN) to simulate DIC data has allowed for the generation of artificial DIC data, particularly in the context of analyzing cracks in materials, improving predictive capabilities in real experiments (Melching et al., 2023). DIC has also found significant application in biomaterials, enabling the measurement of deformations in biological tissues such as muscles and skin, contributing to a better understanding of the biomechanical properties of these materials, such as elasticity and load resistance (Chen et al., 2021). Near-infrared spectroscopy (NIR) has shown great promise in various bio-applications, providing non-invasive and rapid analysis of tissue composition (Beć et al., 2020).

In engineering, DIC has been applied to large structures like bridges and buildings for real-time stress and deformation monitoring, essential for construction safety assessments (Janeliukstis & Chen, 2021). Advances in position registration algorithms now allow subpixel accuracy in image alignment, crucial for high-resolution DIC analyses, improving measurement precision (Chen et al., 2018). Micro-speckle patterns have further enabled deformation analysis at micro- and nano-scales, useful in extreme conditions like high temperatures or corrosion (Dong et al., 2015). Integrating DIC with finite element methods (FEM) enables more detailed modeling of material behavior under load, enhancing predictions of mechanical properties (Chen et al., 2015). DIC allows researchers to detect structural changes, providing valuable insights into mechanical properties under various conditions (Sause, 2016). Especially effective for heterogeneous materials, DIC helps analyze composites and bioinspired materials where traditional methods fall short (Valle et al., 2015). Zhang et al. (2022) used DIC to study fractal patterns in composites, achieving high accuracy in identifying microstructural changes, and DIC has also been effectively used to track crack propagation in complex geological materials, combining experimental data with numerical simulations for improved accuracy (Hou et al., 2024). Additionally, Sause (2016) highlighted the combined use of DIC with visible spectrum spectroscopy, providing insights into materials' spectroscopic and mechanical properties. The visible spectrum (400–700 nm) is crucial for optical analysis, revealing layers and components of materials (Lalena et al., 2020). Different wavelengths enable targeted studies of light-material interactions, such as absorption and scattering, which is vital in materials with complex microstructures (Kohli & Mittal, 2019). Studies (Zhang et al., 2022; Šofer et al., 2023) emphasize wavelengths like 446 nm, 550 nm, and 649 nm, where the cosine nature of signals shows periodic changes in material characteristics, indicating consistency in spectral responses essential for precise optical property measurement. Wavelengths from 657 nm to 765 nm mark the transition from the red spectrum to near-infrared (NIR) (Rogalski, 2003). This range provides a stable response to wavelength changes, underscoring the uniformity of material reactions to light. Such wavelengths are vital in analyzing materials with complex light interactions, like biological samples or composite materials with heterogeneous structures (Van Slyke et al., 1996).

This study is motivated by the need to enhance precision in material analysis through DIC techniques combined with spectroscopic analysis in the visible spectrum. Traditional methods often lack sufficient resolution and accuracy for materials with complex microstructures, especially where subtle optical changes occur. By integrating DIC with multi-wavelength analysis, this work aims to achieve a more detailed understanding of material behavior, enabling precise characterization under various conditions (Sakudo, 2016). The paper begins with DIC principles and visible spectrum analysis, then details the theoretical framework, key wavelengths, and material interactions. Experimental results and discussion follow, focusing on the benefits and limits of the proposed method compared to traditional approaches. Key findings and future research directions are summarized at the end. The code for the proposed method is written in the Matlab software package and is available for testing at <https://github.com/RatkoIV/WHWC-Model->.

Materials and methods

DIC mathematical model

To achieve precise pixel correlation and image segmentation within the spectral range, the proposed methodology employs weighting techniques and harmonic functions through the WHWC (Windowed Harmonic Weighted Correlation) model. This approach integrates classical mathematical methods of image correlation with specific enhancements, including harmonic weighting and the application of a sinusoidal factor. This combination allows for more accurate local analysis, reduces noise impact, and increases robustness across various wavelengths. In this section, the mathematical foundations of the WHWC model and the key equations that ensure its precision and stability in application are explained. We present a detailed step-by-step derivation of these key equations, including their mathematical justification, to make the relationship between these equations and the proposed system accessible, especially for readers without a specialized background. The WHWC model is based on two main factors: harmonic weighting and the sinusoidal function, which are applied to each pixel within an image segment to enhance accuracy. The first phase of developing the mathematical equations for the WHWC model involves harmonic weighting, aimed at suppressing noise by assigning higher weight to central pixels. This weighting is applied according to the position of each pixel (i,j) within the window P_w ensuring local accuracy and emphasizing the central pixels

over the edges, where noise typically dominates. The mathematical definition of harmonic weighting for a pixel (i,j) within a window of size $m \times n$ is given by:

$$W_h(i,j) = \frac{1}{1+d(i,j)}, \quad (1)$$

where $d(i,j)$ is the distance of pixel (i,j) from the center of the window P_ω . This weighting function is designed to give greater value to central pixels within each window compared to edge pixels, contributing to the stability of the correlation coefficient at a local level. In this way, harmonic weighting reduces the influence of edge pixels, which are generally more prone to noise and errors. The next key element of the WHWC model is the sinusoidal function, which introduces additional nonlinearity into the correlation analysis and is particularly useful for analyzing periodic intensity changes within pixels. The sinusoidal function is calculated based on the pixel indices within the window, enabling the model to recognize and analyze complex patterns within the images. The sinusoidal factor $S(i,j)$ for a pixel (i,j) is defined as:

$$S(i,j) = \sin\left(\frac{2\pi(i+j)}{m+n}\right). \quad (2)$$

This function allows for differential weighting of each pixel within the window, especially beneficial in spectral image analysis, where different wavelengths may produce characteristic patterns in pixel intensity distribution. By combining harmonic weighting and the sinusoidal factor, a stable correlation is achieved with reduced noise influence and a robust model response to intensity variations. The correlation coefficient for each window P_ω , using the WHWC model, is calculated as follows:

$$C_{wh}(i,j) = W_h(i,j) \cdot S(i,j) \cdot C(i,j) \quad (3)$$

where $C(i,j)$ is the basic correlation coefficient between corresponding pixels in the reference and analyzed image. This correlation coefficient is adjusted based on the harmonic weighting and sinusoidal factor, ensuring accuracy within local windows and reducing errors originating from noise at the edges. The WHWC model's validation was conducted by comparing results obtained from traditional DIC methods with those obtained using the WHWC model. Correlation coefficients calculated for each wavelength indicated a gradual improvement in stability and accuracy, particularly at wavelengths above 600 nm, where the model showed a performance improvement of approximately 23 to 31% compared to standard methods.

Traditionally, DIC employs basic statistical methods to calculate the correlation between windows (segments) of two images (He et al., 2023). The most commonly used measure is the normalized cross-correlation (NCC) coefficient, which assesses the similarity between two image segments by comparing variations in pixel intensities within the window. The basic formula for NCC is:

$$\rho = \frac{\sum_{i=1}^m \sum_{j=1}^n (I_1(i,j) - \bar{I}_1) \cdot (I_2(i,j) - \bar{I}_2)}{\sqrt{\sum_{i=1}^m \sum_{j=1}^n (I_1(i,j) - \bar{I}_1)^2} \cdot \sqrt{\sum_{i=1}^m \sum_{j=1}^n (I_2(i,j) - \bar{I}_2)^2}} \quad (4)$$

where $I_1(i,j)$ and $I_2(i,j)$ are the pixel intensities in the corresponding windows of the two images, and \bar{I}_1 and \bar{I}_2 are the mean pixel intensities within those windows. However, the basic correlation model may be insufficient for analyses requiring high precision, such as those in spectral analysis where the image is examined at different wavelengths. Therefore, it is necessary to develop advanced mathematical models that incorporate more complex weighting factors and nonlinear functions to enhance the accuracy and robustness of DIC in the analysis of spectral images.

Proposed enhanced mathematical model: WHWC

In response to the need for more precise analysis, a new model called Windowed Harmonic Weighted Correlation (WHWC) has been proposed. This model introduces harmonic weighting factors, which assign greater weight to pixels closer to the center of the window, thereby reducing the influence of edges that may be susceptible to noise and other undesirable effects. Additionally, the WHWC model incorporates a sinusoidal factor that depends on the position of the pixels within the window, allowing for greater flexibility in analyzing different parts of the image. The mathematical definition of WHWC is given by the following formula:

$$\rho = \frac{\sum_{i=1}^m \sum_{j=1}^n W_h(i,j) \cdot [I_1(i,j) \cdot I_2(i,j)] \cdot \sin\left(\frac{\pi(i+j)}{2 \cdot m \cdot n}\right)}{\sqrt{\sum_{i=1}^m \sum_{j=1}^n W_h(i,j) \cdot [I_1(i,j)^2]} \cdot \sqrt{\sum_{i=1}^m \sum_{j=1}^n W_h(i,j) \cdot [I_2(i,j)^2]}} \quad (5)$$

where $W_h(i,j)$ represents the harmonic weighting factor, defined as:

$$W_h(i,j) = \frac{1}{1 + \left(\frac{(i-m)^2 + (j-n)^2}{\sigma^2} \right)} \quad (6)$$

This weighting factor ensures that pixels closer to the center of the window have a greater influence on the overall correlation coefficient, while the sinusoidal factor introduces additional nonlinearity that depends on the pixel position within the window. The sinusoidal factor is crucial for wavelength analysis, as it allows different parts of the image to contribute differently to the overall correlation, which is particularly useful in spectral analysis where different wavelengths may have distinct patterns in pixel intensity distribution.

Advantages of the WHWC model

The WHWC model offers several key advantages compared to traditional correlation models:

- Improved Sensitivity to Local Changes: The introduction of weighting factors allows for better detection of local changes in the image, which is essential for spectral analysis, where changes are often subtle and localized.
- Nonlinear Analysis: The sinusoidal factor introduces nonlinearity, enabling more accurate analysis of complex patterns in images. This approach is particularly useful for analyses where nonlinear behavior patterns are expected, as is the case in spectral analyses of various materials.
- Robustness to Noise: The weighting factors reduce the impact of window edges, which are often affected by noise and other unwanted effects, resulting in greater robustness of the analysis.

Implementation of the WHWC model in DIC

For the purposes of spectral image analysis, the WHWC model can be easily implemented within the framework of standard DIC methods. Instead of using traditional correlation methods, WHWC employs predefined mathematical functions to calculate the correlation coefficient between corresponding windows in the full-spectrum image and the image at a specific wavelength. Given the complexity of the model, WHWC requires greater computational power compared to traditional methods. However, this additional computational demand is justified by the improvements in accuracy and sensitivity of the analysis, which are crucial for advanced spectral analyses where precise and robust results are needed.

Correlation relationship between window index and correlation coefficient

One of the important aspects of the WHWC model is the correlation relationship between the window index and the correlation coefficient. The introduction of the sinusoidal factor, which is a function of the pixel index within the window, allows the model to consider not only the similarity between image segments but also their position within the image. This approach is useful in scenarios where the analysis is position-dependent, as is the case in spectral analysis, where changes in intensity may vary depending on the position within the image. Mathematically, this relationship is represented by the following function:

$$S(i,j) = \sin\left(\frac{\pi}{2} \cdot \frac{i \cdot j}{m \cdot n}\right) \quad (7)$$

where $S(i,j)$ represents the sinusoidal factor that depends on the pixel indices i and j within a window of size $m \times n$. This factor ensures that different parts of the image can contribute differently to the overall correlation, allowing the model to detect and analyze complex patterns within images.

The development of advanced mathematical models for DIC, such as WHWC, represents a significant step forward in the analysis of spectral images. The WHWC model combines the advantages of harmonic weighting factors and nonlinear sinusoidal functions, enabling more precise and robust image analysis at various wavelengths. The implementation of this model can significantly improve outcomes in the analysis of materials and structures, particularly in contexts where it is necessary to analyze changes in pixel intensities with a high level of precision. The introduction of the correlation relationship between window indices and the correlation coefficient provides additional flexibility in the analysis, making this model suitable for a wide range of applications in the field of digital image correlation.

Diagram, flowchart, and algorithm

This section provides an overview of the functionality of the proposed WHWC (Windowed Harmonic Weighted Correlation) model, including a visual representation and algorithmic steps to facilitate the model's implementation and comprehension of its analytical process.

W HWC model workflow diagram

The WHWC model workflow diagram illustrates a step-by-step approach for the image analysis process, showing three primary analytical stages:

- Spectral Image Input: The system receives images captured at various wavelengths across the visible and near-infrared spectrum.
- WHWC Model Application: Harmonic weighting and sinusoidal factors are applied to enhance correlation accuracy within each image segment.
- Results Analysis and Display: Correlation values between pixels in the analyzed windows are evaluated, and the results are presented.

W HWC model flowchart

The flowchart outlines the following steps:

- Initiate Spectral Image Input.
- Image Segmentation into Windows – The image is divided into smaller segments to enable precise local analysis.
- Calculate Harmonic Weighting for Each Window – Weighting is applied to emphasize central pixels in each segment, reducing noise influence.
- Apply the Sinusoidal Factor – This factor is applied to each image to ensure stability and allow for nonlinear analysis.
- Compute Correlation Coefficient – Correlation is calculated between the reference image and the analyzed image.
- Results Analysis and Display – Results are presented through graphs that allow for comparing WHWC model performance with traditional methods.

Algorithm for implementing the WHWC model

The pseudocode for implementing the WHWC model within a DIC system is outlined in the following steps:

1. Input: Set of spectral images $\{S_1, S_2, \dots, S_n\}$
2. For each image S_i in the set:
 - a. Divide the image into windows of size mxn
 - b. For each window P_w in S_i :
 - i. Calculate harmonic weighting $W_h(i,j)$ for each pixel in P_w :

$$W_h(i,j) = \text{harmonic_weight_function}(i, j)$$
 - ii. Apply sinusoidal factor $S(i,j)$ to each pixel in P_w :

$$S(i,j) = \text{sinusoidal_function}(i, j)$$
 - iii. Compute the correlation coefficient between P_w and the corresponding window in the reference image
 - c. Store the correlation coefficient for each window
 3. Display results and analyze the stability of correlation values across the image set
 4. Output: Graph or table with correlation coefficients for all windows and wavelengths

The WHWC model uses harmonic weighted factors and sinusoidal factors to enable robust analysis that remains stable and precise across various wavelengths.

Images in analysis

Wavelengths of 446 nm, 550 nm, and 649 nm encompass key points in the visible spectrum: blue, green, and red light. These colors are primary components recognized by the human eye and are used in material analysis across fields like biology, medicine, and color technology. Wavelengths from 657 nm to 765 nm cover the upper portion of the red spectrum and transition into the near-infrared (NIR) region, a critical shift between visible light and the NIR spectrum, which is utilized in advanced technologies such as biomedical diagnostics, material analysis, and optical communication. These specific wavelengths reveal how materials absorb, reflect, and transmit light, providing information about their physical and chemical properties, and are also applied in standard optical devices for spectral analysis. The images used in this analysis are

characteristic test images commonly applied in the field of DIC, allowing for comparability with other studies. For manuscript optimization, only images corresponding to these wavelengths are shown, while the complete image set is available at <https://sipi.usc.edu/database/>. Figure 1 is an example from the set of 600 images, representing characteristic wavelengths.

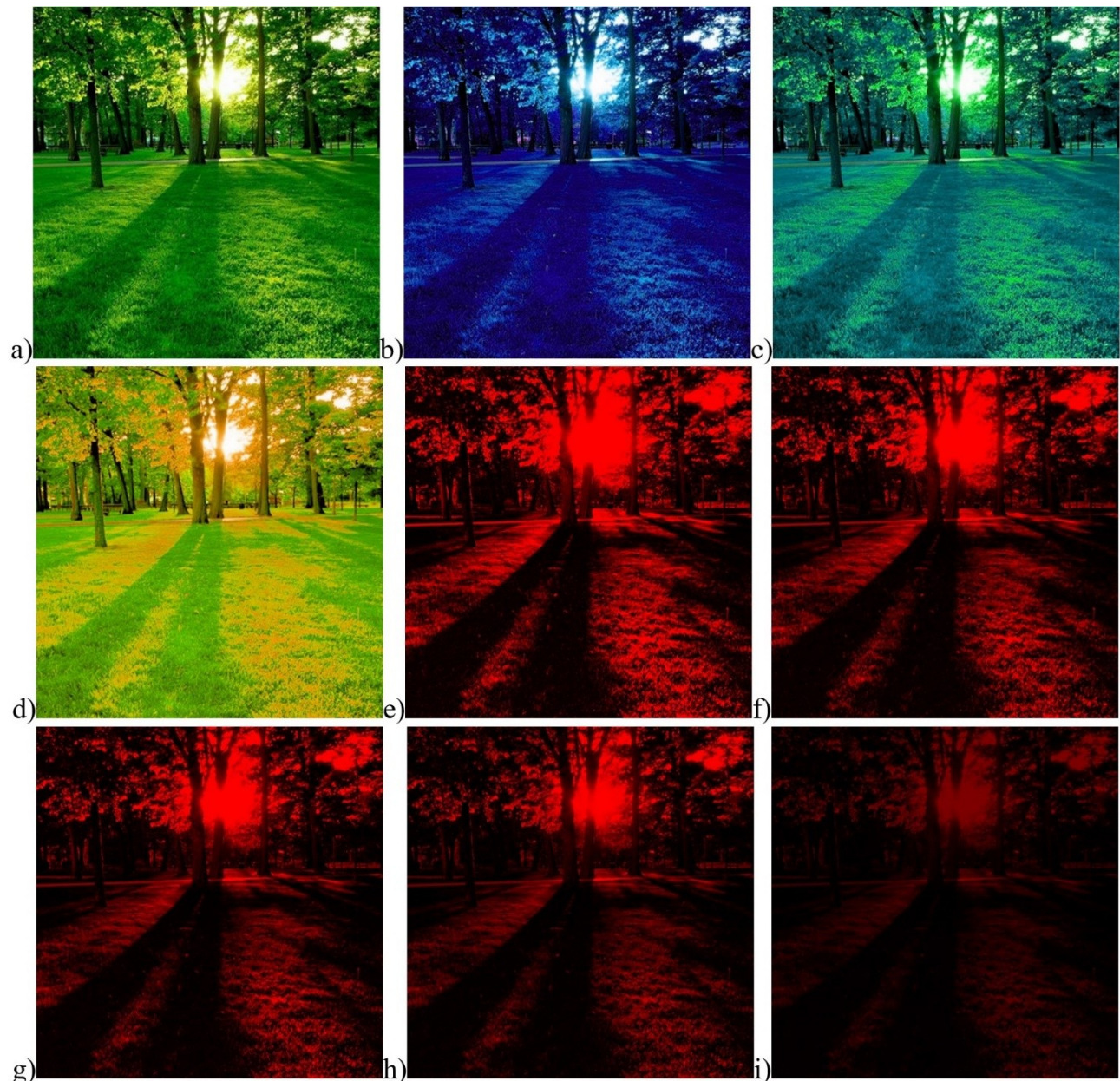


Figure 1. a) The full visible spectrum, filtered at specific wavelengths: b) 446 nm, c) 550 nm, d) 649 nm, e) 657 nm, f) 710 nm, g) 721 nm, h) 750 nm, i) 765 nm.

Results and discussion

In this section, we present an analysis and interpretation of the results obtained through the implementation of the proposed DIC (Digital Image Correlation) model, which integrates the WHWC (Windowed Harmonic Weighted Correlation) model. For this analysis, we used the previously mentioned dataset of 600 spectral images captured across various regions of the visible and near-infrared spectrum. This extensive dataset enabled a more comprehensive examination of the accuracy and stability of the proposed method across a broad spectral range. In our analysis, we compared the performance of the WHWC model with the traditional Normalized Cross-Correlation (NCC) approach, which represents the standard method for comparing image segments in digital correlation. The NCC method uses statistical techniques to assess similarity between two image segments by comparing variations in pixel intensity within the segment.

However, it is known that NCC can have limited precision under high accuracy requirements, such as analyses of spectral images with varying wavelengths, where intensity changes occur at a microscopic level and are often susceptible to noise. Figure 2 illustrates the improvements of the proposed WHWC model compared to the NCC method across the entire visible spectrum. The results demonstrate a significant increase in stability and accuracy across all analyzed wavelength ranges, with improvements ranging from 23% to 31% over the NCC method. These improvements are quantified by the average correlation coefficients obtained using the WHWC method in comparison to the NCC method, where the relative increase is expressed by the formula:

$$\text{Improvement}(\%) = \frac{\text{Correlation coefficient (WHWC)} - \text{Correlation coefficient (tradicional)}}{\text{Correlation coefficient (tradicional)}} \quad (8)$$

This formula allows for direct comparison of average correlation coefficient values between both approaches, further confirming that the WHWC model contributes to the field of DIC in terms of stability and accuracy across varying wavelengths. Performance enhancements in the WHWC model are also evident in the stability of results across different window indices. Traditional DIC analysis methods, such as NCC, often exhibit fluctuations in correlation coefficients depending on the position of the window within the image, which can contribute to increased noise and reduced result reliability. The WHWC model employs harmonic weighting and a sinusoidal factor that collectively mitigate these fluctuations, thereby achieving a more stable correlation across all image windows. Mathematical stability is supported by the low contribution of higher-order terms in the polynomial approximation of the correlation coefficients, which further enhances the robustness of the WHWC method. These results suggest that the WHWC model possesses an exceptional capability for detecting and analyzing complex relationships between image segments at different wavelengths. The model's stability has proven particularly effective at higher wavelengths, above 600 nm, where performance improvement gradually increases, which can be linked to the enhanced interaction potential of these wavelengths with various materials.

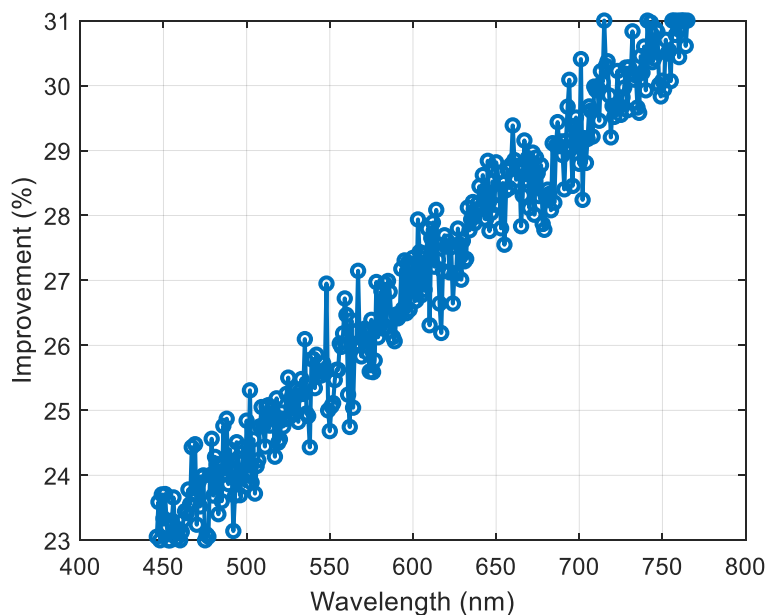


Figure 2. Improvement of the Proposed WHWC Method Across the Visible Spectrum.

The improvement of the WHWC model increases with wavelength because images with longer wavelengths have a greater potential for processing due to their enhanced ability to interact with materials. As the wavelength increases, images become less susceptible to noise and dispersion, allowing the WHWC model to more effectively detect and analyze changes in material structure (Ivković, 2020). This stability and increased informativeness at longer wavelengths make the model more suitable for precise analysis, resulting in a gradual improvement in performance across the entire visible spectrum.

One of the critical advantages of our WHWC model is its stability across different window indices. In traditional DIC methods, the correlation coefficient often fluctuates significantly depending on the position of the window in the image. These fluctuations can introduce noise and reduce the reliability of the correlation analysis, especially in heterogeneous materials or when the image contains areas with varying

texture or intensity. Our method addresses these issues by incorporating harmonic weighting and a sinusoidal factor, which collectively smooth out the variations in correlation across different windows. The stability is mathematically supported by the low contribution of higher-order terms in the polynomial approximation of the correlation coefficients. As shown by the general polynomial $P(x) = -0.0006x + 0.3455$. This suggests that the relationship between the window position and the correlation coefficient is primarily linear, with a strong constant component. The negative linear term $-0.0006x$ introduces a slight decline as the window index increases, but this effect is minimal, which contributes to the overall stability of the method. To further understand the improvements, we can decompose the polynomial into its components and analyze their contributions:

➤ Constant term (0.3455): This term represents the baseline correlation coefficient, independent of the window index. It is the dominant factor in the polynomial, indicating that the correlation coefficient remains consistently high across different windows.

➤ Linear term ($-0.0006x$): The linear term introduces a slight negative slope, which suggests a gradual decrease in the correlation coefficient as the window index increases. However, this decrease is minor, indicating that the correlation coefficient does not fluctuate wildly as the window moves across the image.

The stability can be further understood by considering the variance in the correlation coefficients across different windows. A stable method will have a low variance, indicating that the correlation coefficients are similar regardless of the window's position. Mathematically, this can be expressed as:

$$\sigma^2 = \frac{1}{N} \sum_{i=1}^N (\rho_i - \bar{\rho})^2 \quad (9)$$

where, σ^2 - is the variance of the correlation coefficients, ρ_i - is the correlation coefficient for the i -th window, $\bar{\rho}$ - is the mean correlation coefficient, N - is the total number of windows. Our method shows a significantly lower variance compared to traditional methods, which is indicative of the WHWC model's ability to maintain high correlation coefficients across different windows. This stability is essential for applications that require reliable image analysis, such as in material science or biomedical imaging.

Oscillations in correlation coefficients

Despite the overall stability, there are some oscillations in the correlation coefficients observed for different window indices. These oscillations are captured by the sinusoidal factor introduced in the WHWC model:

$$\text{Sin_f factor} = \sin\left(\frac{\pi}{2} \cdot \frac{X \cdot Y}{m \cdot n}\right) \quad (10)$$

This factor introduces a controlled non-linearity into the correlation calculation, which allows the model to better account for periodic variations in the image data, such as those caused by repeating patterns or textures. The oscillations in the correlation coefficients are reflective of the underlying structure of the image, with the WHWC model accurately capturing these variations. The presence of these oscillations suggests that while the correlation coefficients are stable overall, the WHWC model is sensitive enough to detect subtle changes in the image data that might be missed by more linear methods. This sensitivity is particularly important in applications where detecting small differences in image segments is critical, such as in the detection of defects or anomalies.

As can be observed in Figure 3, which presents the graphs for the wavelengths 446 nm, 550 nm, and 649 nm, the results indicate that these graphs are nearly identical and exhibit a cosine nature. This phenomenon may point to several key aspects:

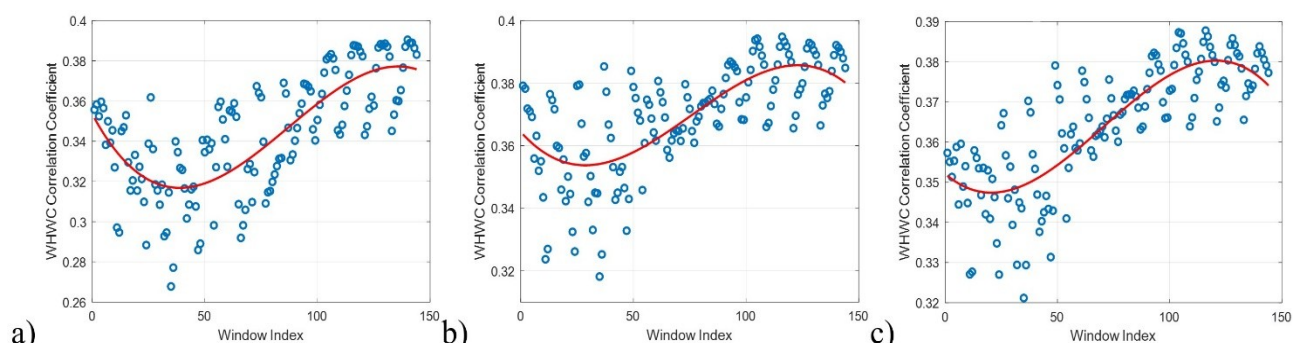


Figure 3. WHWC Correlation for a) 446 nm, b) 550 nm, c) 649 nm, with 3rd degree polynomial.

➤ **Symmetry and Periodicity:** The cosine nature of the graphs suggests the presence of symmetrical, periodic changes in image characteristics when analyzed at these wavelengths. This may indicate that the images being analyzed are subject to regular, cyclical variations, which are characteristic of structures or patterns that repeat within the image. In optical systems, cosine signals often reflect regular interference patterns or periodic changes in illumination, which may be associated with regular structures in the material or texture of the analyzed object.

➤ **Signal Uniformity:** The identical nature of the graphs across different wavelengths suggests that there is a unique structure or property of the image that is consistent in these parts of the spectrum. This could mean that the materials or objects in the image reflect or transmit light in a similar manner at all these wavelengths. Interestingly, this phenomenon suggests that these wavelengths might be too similar in terms of their interaction with the analyzed material, which could reduce their effectiveness in distinguishing different structures or phases within the image.

➤ **Significance of Wavelength Range:** The wavelengths from 446 nm (blue light), through 550 nm (green light), to 649 nm (red light), cover a significant portion of the visible spectrum. If the graphs are identical, it can be concluded that the material's reactions within this spectrum are consistent, suggesting that this analysis may not reveal additional information over a broader spectrum. This result may indicate that the material is relatively uniform in its spectral response to visible light or that the objects analyzed in the image behave as homogeneous within this spectrum.

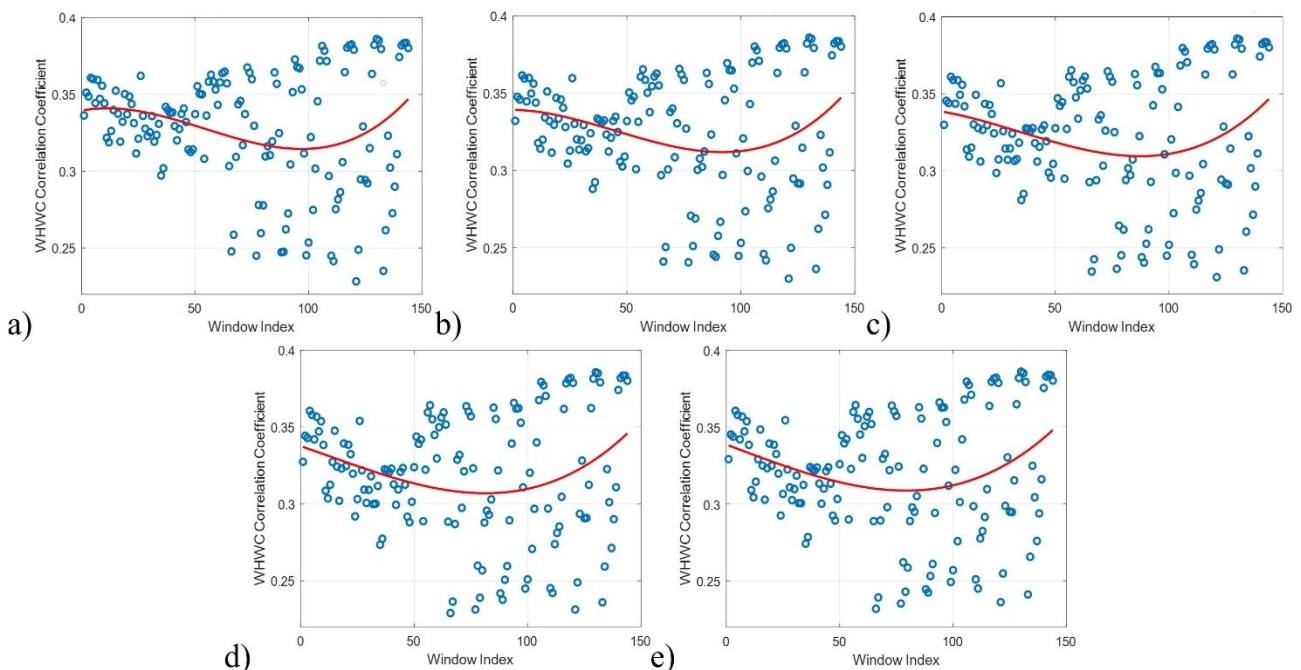


Figure 4. WHWC Correlation for a) 657 nm, b) 710 nm, c) 721 nm, d) 750 nm, e) 765 nm, with 3rd degree polynomial.

Wavelengths in the range of 657 nm to 765 nm fall within the upper portion of the visible spectrum and the transition to the near-infrared (NIR) region. Wavelengths from 657 nm to around 700 nm are situated in the red part of the visible spectrum, with light in this range appearing red. The range from 700 nm to 765 nm represents the transition from visible red light to the near-infrared (NIR) region. Light near 700 nm is on the boundary between visible red and NIR light, while wavelengths up to 765 nm belong to the initial part of the NIR spectrum. As shown in Figure 4, the resulting graphs are nearly identical, indicating a stable or uniform system response to changes in wavelength within this range. This may be significant for highlighting the specificity of the transition zone between visible red light and the beginning of the near-infrared (NIR) spectrum.

The generalized conclusion for the entire visible spectrum, based on the research results, emphasizes the exceptional advantage of the proposed method in analyzing the stability and uniformity of system responses to changes in wavelength. The proposed method demonstrates high reliability and consistency in identifying spectral characteristics across the entire visible spectrum, from blue to red light, and the transition to the near-infrared region (NIR). One of the key advantages of this method is its ability to precisely detect and analyze the spectral response of materials across different wavelength ranges, enabling the identification of

uniform and specific patterns in spectral characteristics. This consistency in wavelength analysis underscores the robustness of the method, making it superior to traditional approaches that may be more sensitive to variations in wavelength. Furthermore, the method provides a clear picture of how different materials or structures behave across the spectrum, allowing for a deeper understanding of their optical properties. The ability of the method to generate stable and predictable results across the entire wavelength spectrum opens new possibilities for applications in fields where precise spectral analysis is required, such as materials science, biomedical research, and optical detection.

Comparison with existing methods and contribution of the WHWC model

Approaches based on Digital Image Correlation (DIC) in the analysis of deformations and stresses have significantly evolved to cover various applications, materials, and technological demands. Piekarczyk et al. (2022) explored the use of hyperspectral data combined with RGB analysis to identify three types of polyphagous fungi. Using machine learning methods, particularly the 'extreme boosting machine' technique, the authors achieved high classification accuracy through hyperspectral analysis, especially in the short-wave infrared (SWIR) and visible spectrum. In the context of spectral characterization models, Li et al. (2021) developed an algorithm for fusing visible and near-infrared (NIR) images, relying on reflection and transmission weighting models. This approach preserves spectral characteristics without color distortion, offering a significant step toward more accurate spectral analysis for natural scenes, although it brings complexity in data processing. Additionally, Meng et al. (2022) investigated a new optical method based on nanoparticles that detect stress changes via shifts in emission wavelengths. Other approaches focused on fusing visible and near-infrared images, such as reflection and transmission weighting models, have preserved spectral characteristics well but at the cost of increased processing complexity (Li et al., 2021). Their 'strain-sensing smart skin' (S4) system achieves high spectral uniformity with minimal calibration requirements at high temperatures and demonstrates notable precision when monitoring damage in materials like concrete and acrylic compared to traditional DIC methods. Yu and Pan (2021) described the application of DIC methods at high temperatures, tackling challenges such as image saturation and contrast loss due to thermal radiation. The proposed method uses customized speckle patterns and techniques to minimize the effects of thermal radiation and air distortion, making it applicable in demanding environments such as industrial metallurgy. Furthermore, the application of DIC methods for large structures such as bridges and buildings has been enabled through research by Janeliukstis and Chen (2021), who identified key challenges and benefits when applied to testing large composite structures. By optimizing position registration algorithms and using DIC for non-contact stress measurements, they achieved subpixel accuracy, which is essential for real-time deformation measurements. Similarly, Liu and Wei (2024) investigated damage mechanisms in concrete beams embedded with sensors, combining DIC with acoustic emissions (AE) for comprehensive damage assessment, demonstrating this approach's potential for sensor-embedded structures. The use of DIC combined with near-infrared spectroscopy for tissue characterization, as described by Afara et al. (2021), allows for non-destructive analysis of biological tissues, which is particularly valuable in medical and biomechanical research. Applying this technique in the assessment of elastin and collagen offers additional insights into tissue structural properties, complementing standard tissue analysis methods.

The WHWC (Windowed Harmonic Weighted Correlation) method offers a comprehensive approach to spectral data analysis, effectively addressing challenges characteristic of digital image correlation (DIC) and related techniques. First, the harmonic weighting employed by WHWC significantly reduces noise in edge analyses, where pixels are most prone to errors and intensity variations. This ensures a more stable result, essential in microscopic structural analyses where it is important to maintain natural spectral characteristics without the use of additional materials, such as nanoparticles. Unlike methods that require specialized sensors, WHWC adapts to the natural spectral properties of materials, enabling direct analysis without calibration needs, which ensures speed and reliability—especially valuable in demanding environments. On the other hand, algorithms for fusing visible and NIR images often face challenges such as color distortion and preservation of spectral characteristics. The WHWC method overcomes these issues by employing harmonic weighting, achieving a natural integration across different spectral ranges with a stable spectroscopic response. Unlike algorithms that require additional layers of processing and correction, WHWC directly analyzes subtle intensity changes without extra computational load, facilitating real-time application with reduced processing complexity. Methods that apply hyperspectral data in combination with machine learning algorithms demonstrate high accuracy but come with significant resource and processing demands.

In contrast, WHWC achieves a comparable level of precision through a simpler algorithm, enabling efficient spectral data analysis without advanced processing techniques. The harmonic weighting in WHWC optimizes accuracy compared to conventional DIC approaches, as it better detects subtle changes at the edges, which is crucial in detailed spectral analyses. An additional advantage of WHWC is its resilience to challenges related to high temperatures, such as increased thermal radiation and reduced contrast due to heat. While traditional methods face issues in these conditions, WHWC provides more stable results by reducing noise effects and adapting to various environmental conditions, making it extremely useful in industrial and scientific environments where high temperatures and other challenging conditions are common.

Implications for practical applications

The improvements and stability offered by the WHWC model have significant implications for various practical applications. In fields such as material science, where precise image correlation is crucial for analyzing material properties and behavior under different conditions, the WHWC model provides a more reliable tool (Santos et al., 2020). The model's ability to maintain high correlation coefficients across different windows ensures that analyses are not skewed by local variations in the image, leading to more accurate results. In biomedical imaging, where detecting small changes in tissues or cells is essential, the WHWC model's sensitivity to oscillations and its overall stability make it an ideal choice. The model's ability to handle images with varying textures and intensities without losing accuracy ensures that subtle changes are detected, which is critical for early diagnosis and treatment planning. Similar studies have combined advanced signal pre-processing techniques with optimal band selection algorithms in the Vis-NIR spectrum to predict chemical properties such as soil organic matter content, demonstrating the power of spectral analysis beyond imaging tasks (Zhang et al., 2020).

Limitations and future work

While the WHWC model shows improvements over traditional methods, there are some limitations to consider. The model's reliance on harmonic weighting and sinusoidal factors means that it may not perform as well in images with very high noise levels or in cases where the image data is highly irregular. Additionally, the computational complexity of the WHWC model is higher than that of traditional methods, which may be a consideration in real-time applications where processing speed is critical. Future work could focus on optimizing the WHWC model for faster processing while maintaining its stability and accuracy. Additionally, exploring alternative weighting schemes or incorporating machine learning techniques could further enhance the model's performance, particularly in challenging imaging conditions. Recent advances in transfer learning have shown potential in environmental spectral analysis, suggesting similar methods could be explored to improve adaptability of the WHWC model (Yang et al., 2023).

Conclusion

This study highlights the WHWC model as a significant enhancement to traditional Digital Image Correlation (DIC) methods, improving stability and precision in spectral image analysis across visible and near-infrared ranges. By integrating harmonic weighting and a sinusoidal component, the model effectively reduces noise and increases sensitivity to localized changes, outperforming the Normalized Cross-Correlation (NCC) method. Testing on 600 spectral images across diverse materials validated its strengths through mathematical, visual, and descriptive analyses. WHWC shows potential for applications in material science, environmental monitoring, and biomedical imaging, with future work aimed at improving computational efficiency and integrating machine learning techniques.

References

Šofer, M., Šofer, P., Pagáč, M., Volodarskaja, A., Babiuch, M., & Gruň, F. (2023). Acoustic Emission Signal Characterisation of Failure Mechanisms in CFRP Composites Using Dual-Sensor Approach and Spectral Clustering Technique. *Polymers*, 15(1), 47. <https://doi.org/10.3390/polym15010047>

Afara, I. O., Shaikh, R., Nippolainen, E., Querido, W., Torniainen, J., Sarin, J. K., Kandel, S., Pleshko, N., & Töyräs, J. (2021). Characterization of connective tissues using near-infrared spectroscopy and imaging. *Nature Protocols*, 16, 1297–1329. <https://doi.org/10.1038/s41596-020-00468-z>

Beć, K. B., Grabska, J., & Huck, C. W. (2020). Near-infrared spectroscopy in bio-applications. *Molecules*, 25(12), 2948. <https://doi.org/10.3390/molecules25122948>

Chen, T. Y. F., Dang, N. M., Wang, Z. Y., Chang, L. W., Ku, W. Y., Lo, Y. L., & Lin, M. T. (2021). Use of digital image correlation method to measure bio-tissue deformation. *Coatings*, 11(8), 924. <https://doi.org/10.3390/coatings11080924>

Chen, Z., Quan, C., Zhu, F., & He, X. (2015). A method to transfer speckle patterns for digital image correlation. *Measurement Science and Technology*, 26(9), 095201. <https://doi.org/10.1088/0957-0233/26/9/095201>

Chen, Z., Shao, X., Xu, X., & He, X. (2018). Optimized digital speckle patterns for digital image correlation. *Applied Optics*, 57(4), 884-893. <https://doi.org/10.1364/AO.57.000884>

Dong, Y., Kakisawa, H., & Kagawa, Y. (2015). Development of microscale pattern for digital image correlation up to 1400°C. *Optics and Lasers in Engineering*, 68, 7-15. <https://doi.org/10.1016/j.optlaseng.2014.12.003>

Duan, X., Xu, H., Dong, R., Lin, F., & Huang, J. (2023). Digital image correlation based on convolutional neural networks. *Optics and Lasers in Engineering*, 160, 107234. <https://doi.org/10.1016/j.optlaseng.2022.107234>

Hansen, R. S., Waldram, D. W., & Thai, T. Q. (2021). Super resolution digital image correlation (SR-DIC): An alternative to image stitching at high magnifications. *Experimental Mechanics*, 61, 1351–1368. <https://doi.org/10.1007/s11340-021-00729-2>

He, X., Zhou, R., Liu, Z., Yang, S., Chen, K., & Li, L. (2023). Review of research progress and development trend of digital image correlation. *Multidiscipline Modeling in Materials and Structures*, 20(1), 81-114. <https://doi.org/10.1108/MMMS-07-2023-0242>

Hou, Z., Yuan, R., Chen, Y., & Sun, W. (2024). Crack propagation process in double-flawed granite under compression using digital image correlation method and numerical simulation. *Scientific Reports*, 14, 21424. <https://doi.org/10.1038/s41598-024-72302-5>

Ivković, R. (2020). *New model of partial filtering in implementation of algorithms for edge detection and digital image segmentation*. [Doctoral thesis, Faculty of Technical Sciences, K. Mitrovica, Serbia]. <https://nardus.mpn.gov.rs/handle/123456789/12374>

Janeliukstis, R., & Chen, X. (2021). Review of digital image correlation application to large-scale structures. *Composite Structures*, 271, 114143. <https://doi.org/10.1016/j.compstruct.2021.114143>

Kohli, R., & Mittal, K. L. (2019). Characterization of surface contaminants and features. In *Developments in Surface Contamination and Cleaning* (Vol. 12, pp. 107-158). Elsevier. <https://doi.org/10.1016/B978-0-12-816081-7.00004-8>

Lalena, J. N., Cleary, D. A., & Duparc, O. H. (2020). Optical properties of materials. In *Principles of Inorganic Materials Design* (3rd ed., pp. 425-447). Wiley. <https://doi.org/10.1002/9781119486879.ch9>

Li, Z., Hu, H.-M., Zhang, W., Pu, S., & Li, B. (2021). Spectrum characteristics preserved visible and near-infrared image fusion algorithm. *IEEE Transactions on Multimedia*, 23, 306-319. <https://doi.org/10.1109/TMM.2020.2978640>

Liu, C., & Wei, Y. (2024). Experimental investigation on damage of concrete beam embedded with sensor using acoustic emission and digital image correlation. *Construction and Building Materials*, 423, 135887. <https://doi.org/10.1016/j.conbuildmat.2024.135887>

Melching, D., Schultheis, E., & Breitbarth, E. (2023). Generating artificial displacement data of cracked specimen using physics-guided adversarial networks. *arXiv*. <https://arxiv.org/pdf/2303.15939v3.pdf>

Meng, W., Pal, A., Bachilo, S. M., Bruce, R. W., & Satish, N. (2022). Next-generation 2D optical strain mapping with strain-sensing smart skin compared to digital image correlation. *Scientific Reports*, 12, 11226. <https://doi.org/10.1038/s41598-022-15332-1>

Piekarczyk, J., Andrzej, W., Marek, W., Jarosław, J., Katarzyna, S., Natalia, Ł.-S., Ilona, Ś., & Katarzyna, P. (2022). Machine learning-based hyperspectral and RGB discrimination of three polyphagous fungi species grown on culture media. *Agronomy*, 12(8), 1965. <https://doi.org/10.3390/agronomy12081965>

Rogalski, A. (2003). Infrared detectors: Status and trends. *Progress in Quantum Electronics*, 27(2-3), 59-210. [https://doi.org/10.1016/S0079-6727\(02\)00024-1](https://doi.org/10.1016/S0079-6727(02)00024-1)

Sakudo, A. (2016). Near-infrared spectroscopy for medical applications: Current status and future perspectives. *Clinica Chimica Acta*, 455, 181-188. <https://doi.org/10.1016/j.cca.2016.02.009>

Santos, U. J., de Melo Demattê, J. A., Menezes, R. S. C., Dotto, A. C., Guimarães, C. C. B., Alves, B. J. R., Sampaio, D. C. P., & Barretto, E. V. S. (2020). Predicting carbon and nitrogen by visible near-infrared (Vis-NIR) and mid-infrared (MIR) spectroscopy in soils of Northeast Brazil. *Geoderma Regional*, 23, e00333. <https://doi.org/10.1016/j.geodrs.2020.e00333>

Sause, F. M. (2016). *In situ monitoring of fiber-reinforced composites: Theory, methods, and applications*. Springer.

Valle, V., Hedan, S., Cosenza, P., Fauchille, A. L., & Berdjane, M. (2015). Digital image correlation development for the study of materials including multiple crossing cracks. *Experimental Mechanics*, 55(2), 379-391. <https://doi.org/10.1007/s11340-014-9948-1>

Van Slyke, S. A., Chen, C. H., & Tang, C. W. (1996). Organic electroluminescent devices with improved stability. *Applied Physics Letters*, 69(15), 2160-2162. <https://doi.org/10.1063/1.117151>

Yang, J., Tao, J. L., & Franck, C. (2021). Smart digital image correlation patterns via 3D printing. *Experimental Mechanics*, 61, 1181–1191. <https://doi.org/10.1007/s11340-021-00720-x>

Yang, Y., Qinfang, C., Rongjie, C., Aidi, H., & Yanting, W. (2023). Retrieval of soil heavy metal content for environment monitoring in mining area via transfer learning. *Sustainability*, 15(15), 11765. <https://doi.org/10.3390/su151511765>

Yu, L., & Pan, B. (2021). Overview of high-temperature deformation measurement using digital image correlation. *Experimental Mechanics*, 61, 1121–1142. <https://doi.org/10.1007/s11340-021-00723-8>

Zhang, X., Zhu, H., Lv, Z., Zhao, X., Wang, J., & Wang, Q. (2022). Investigation of biaxial properties of CFRP with the novel-designed cruciform specimens. *Materials*, 15(19), 7034. <https://doi.org/10.3390/ma15197034>

Zhang, Z., Ding, J., Zhu, C., & Wang, J. (2020). Combination of efficient signal pre-processing and optimal band combination algorithm to predict soil organic matter through visible and near-infrared spectra. *Molecular and Biomolecular Spectroscopy*, 240, 118553. <https://doi.org/10.1016/j.saa.2020.118553>